

Highly Active Iridium Catalysts for Alkane Dehydrogenation. Synthesis and Properties of Iridium Bis(phosphine) Pincer Complexes Based on Ferrocene and Ruthenocene

Sergey A. Kuklin,[†] Alexey M. Sheloumov,[†] Fedor M. Dolgushin,[†] Mariam G. Ezernitskaya,[†] Alexander S. Peregudov,[†] Pavel V. Petrovskii,[†] and Avthandil A. Koridze*,^{†,‡}

A.N. Nesmeyanov Institute of Organoelement Compounds, Russian Academy of Sciences, 28 Vavilov Street, 119991 Moscow, Russian Federation, and I. Javakhishvili Tbilisi State University, 1 Chavchavadze Avenue, 380028 Tbilisi, Georgia

Received August 7, 2006

Novel bis(phosphine) pincer complexes of iridium based on ferrocene and ruthenocene have been synthesized. The reaction of 1,3-bis((di-*tert*-butylphosphino)methyl)metallocenes [t-BuP,CH,P^M] (M = Fe, **10**; M = Ru, **13**) with [Ir(COE)₂Cl]₂ in refluxing toluene leads to the corresponding chloro-hydrido pincer complexes as a mixture of H-*endo*- (M = Fe, **11**; M = Ru, **14**) and H-*exo*-IrH(Cl)[t-BuP,C,P^M] (M = Fe, **12**; M = Ru, **15**) isomers. Treatment of compounds **11**, **12** and **14**, **15** with NaH in hot cyclooctane generates corresponding dihydrido complexes IrH₂[t-BuP,C,P^M] (M = Fe, **6**; M = Ru, **7**). Reactivity of the chelated iridium atom in hydrido-iridium pincer complexes and oxidation centered at the iron atom of ferrocene-based pincer complexes were studied. Complexes H-*exo*-IrH(Cl)(CO)[t-BuP,C,P^{Fe}] (**20**), Ir(CO)[t-BuP,C,P^{Fe}] (**21**), and Ir(CO)[2,6-(t-Bu₂PO)₂C₆H₃] (**30**) were characterized by X-ray crystallography. On the basis of ν_{CO} values for carbonyl iridium derivatives, electronic characteristics of the corresponding fragments {Ir[t-BuP,C,P^M]}ⁿ (n = 0, +1) were elucidated. Complexes **6** and **7** reveal unprecedented catalytic activity in cyclooctane dehydrogenation in the presence of *tert*-butylethylene as a hydrogen acceptor: turnover numbers 3300, 2571, and 1843 were obtained for **6**, **7**, and the known complex IrH₂[2,6-(t-Bu₂PO)₂C₆H₃] (**4c**), respectively, at 180 °C for 8 h. The high catalytic activity for **6** and **7** and the difference in the catalytic activity of these “isostructural” complexes are discussed in terms of steric and electronic effects.

Introduction

Selective functionalization of alkanes and unactivated alkyl groups is one of the most significant tasks of organic chemistry and homogeneous catalysis.¹ Among the known alkane functionalization processes, catalytic alkane dehydrogenation² is a potentially significant reaction since it provides access to olefins that are major organic feedstock used in a variety of industrial processes. Current heterogeneous processes for alkane dehydrogenation operate at high temperatures (400–600 °C),³ and the development of homogeneous processes is attractive from the selectivity and energy efficiency points of view.

Presently the most active and robust homogeneous catalysts for alkane dehydrogenation are benzene- and anthracene-based

bis(phosphine) and bis(phosphinite) P,C,P pincer complexes of iridium, **1–5** (Chart 1).

The high thermal stability of iridium catalysts allows transfer dehydrogenation of alkanes in the presence of *tert*-butylethylene or norbornene as a sacrificial hydrogen acceptor at 100–200 °C;^{1b,c,4} acceptorless dehydrogenation^{4g,h,5} may be achieved using complexes **2**, **5**, and the most stable anthraphos pincer complex, **3**. Although impressive progress has been achieved, there are some problems that preclude practical application of the above iridium pincer complexes. Thus, the rates of alkane dehydrogenation are still insufficient. In addition, product inhibition and isomerization of initially formed α -olefins into internal isomers take place. It is obvious that a search for approaches to the design of novel pincer systems remains a challenging goal.

* Corresponding author. E-mail: koridze@ineos.ac.ru.

[†] A.N. Nesmeyanov Institute of Organoelement Compounds.

[‡] I. Javakhishvili Tbilisi State University.

(1) For reviews see: (a) Labinger, J. A.; Bercaw, J. E. *Nature* **2002**, *417*, 507–514. (b) Crabtree, R. H. *J. Chem. Soc., Dalton Trans.* **2001**, 2437–2450. (c) Jensen, C. M. *Chem. Commun.* **1999**, 2443–2449. (d) Dyker, G. *Angew. Chem., Int. Ed.* **1999**, *38*, 1699–1712. (e) Sen, A. *Acc. Chem. Res.* **1998**, *31*, 550–557.

(2) (a) Crabtree, R. H.; Mihelcic, J. M.; Quirk, J. M. *J. Am. Chem. Soc.* **1979**, *101*, 7738–7740. (b) Baudry, M. J.; Ephritikine, M.; Felkin, H.; Holmes-Smith, R. J. *Chem. Soc., Chem. Commun.* **1983**, 788–789. (c) Baudry, M. J.; Crabtree, R. H.; Parnell, C. P.; Uriarte, R. J. *Organometallics* **1984**, *3*, 816–817. (d) Burk, M. W.; Crabtree, R. H. *J. Am. Chem. Soc.* **1987**, *109*, 8025–8032. (e) Maguire, J. A.; Goldman, A. S. *J. Am. Chem. Soc.* **1991**, *113*, 6706–6708.

(3) (a) Wieseman, P. *Petrochemicals*; Ellis Horwood: Chichester, England, 1986; pp 90–91. (b) Weissmehl, K.; Arpel, H.-J. *Industrial Organic Chemistry*; Wiley VCH: Weinheim, Germany, 2003; pp 59–89.

(4) (a) Gupta, M.; Hagen, C.; Flesher, R. J.; Kaska, W. C.; Jensen, C. M. *Chem. Commun.* **1996**, 2083–2084. (b) Gupta, M.; Hagen, C.; Kaska, W. C.; Cramer, R. E.; Jensen, C. M. *J. Am. Chem. Soc.* **1997**, *119*, 840–841. (c) Liu, F.; Pak, E. B.; Singh, B.; Jensen, C. M.; Goldman, A. S. *J. Am. Chem. Soc.* **1999**, *121*, 4086–4087. (d) Göttker-Schnetmann, I.; White, P.; Brookhart, M. *J. Am. Chem. Soc.* **2004**, *126*, 1804–1811. (e) Göttker-Schnetmann, I.; White, P.; Brookhart, M. *Organometallics* **2004**, *23*, 1766–1776. (f) Göttker-Schnetmann, I.; Brookhart, M. *J. Am. Chem. Soc.* **2004**, *126*, 9330–9338. (g) Morales-Morales, D.; Redon, R.; Yung, C.; Jensen, C. M. *Inorg. Chim. Acta* **2004**, *357*, 2953–2956. (h) Zhu, K.; Achord, P. D.; Zhang, X.; Krogh-Jespersen, K.; Goldman, A. S. *J. Am. Chem. Soc.* **2004**, *126*, 13044–13053.

(5) (a) Xu, W.-W.; Rosini, G. P.; Gupta, M.; Jensen, C. M.; Kaska, W. C.; Krogh-Jespersen, K.; Goldman, A. S. *Chem. Commun.* **1997**, 2273–2274. (b) Liu, F.; Goldman, A. S. *Chem. Commun.* **1999**, 655–656. (c) Haelnel, M.; Oevers, S.; Angermund, K.; Kaska, W. C.; Fan, H.-J.; Hall, M. B. *Angew. Chem., Int. Ed.* **2001**, *40*, 3596–3600.

Chart 1

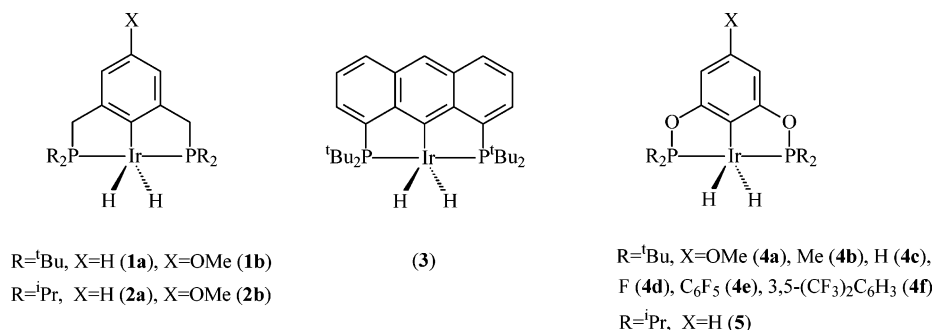
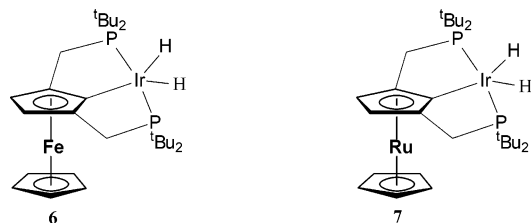


Chart 2



To test catalytic potential of conceptually novel binuclear metallocene-based pincer complexes, we undertook a study of catalytic properties of complexes IrH₂[{2,5-(^tBu₂PCH₂)₂C₅H₂}-M(C₅H₅)] (IrH₂[^t-Bu₂P,C,P^M], M = Fe, **6**; M = Ru, **7**), generated from the corresponding chloro-hydrido iridium complexes⁶ (Chart 2).

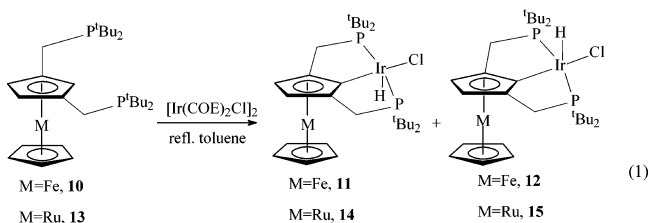
Since catalytic activity of iridium P,C,P pincer complexes should depend on the accessibility of the iridium center to substrate and electronic properties of the Ir[P,C,P] fragment, it was desirable to possess X-ray diffraction data on the steric environment of the Ir atom in metallocene-based pincer complexes, as well as electronic characteristics of the Ir-[^RP,C,P^M] fragments. Unfortunately, we failed to prepare single crystals for complexes IrH₂[^RP,C,P^M] and IrH₄[^RP,C,P^M] suitable for an X-ray diffraction study. For this reason, we propose that the chloropalladium PdCl[^RP,C,P^{Fe}] (R = ⁱPr, **8a**; R = ^tBu, **8b**) and tetrahydroboratopalladium Pd(BH₄)[^RP,C,P^{Fe}] (R = ⁱPr, **9a**; R = ^tBu, **9b**) complexes can be considered as model compounds.⁷ The X-ray diffraction data of **8a,b** and **9b** revealed some interesting features, especially concerning the steric environment of the chelated metal atom.

In the course of our study of iridium P,C,P pincer complexes based on ferrocene, some of these complexes were characterized by X-ray diffraction. On the basis of ν_{CO} values for carbonyl iridium derivatives, electronic characteristics of the corresponding fragments {Ir[^t-Bu₂P,C,P^M]}ⁿ (*n* = 0, +1) were elucidated. In this paper we report the preparation of ferrocene- and ruthenocene-based hydrido iridium pincer complexes, chemical transformations at the chelated iridium atom, and redox reactions centered at the Fe atom of the ferrocene-based pincer complexes. We also report here our *initial studies* of catalytic properties of iridium metallocene-based pincer complexes **6** and **7** in transfer dehydrogenation of cyclooctane (COA) with *tert*-butylethylene (TBE) as a hydrogen acceptor. These complexes reveal an unprecedented level of catalytic dehydrogenation activity.

Results and Discussion

1. Synthesis and Characterization of Metallocene-Based Chloro-Hydrido Iridium Complexes. 1.1. Synthesis of Chloro-Hydrido Complexes.

The reaction of ferrocene diphosphine [^t-Bu₂P,C,P^{Fe}] (**10**) with [Ir(COE)₂Cl]₂ in refluxing toluene gave a mixture of two isomeric complexes, IrH(Cl)[^t-Bu₂P,C,P^{Fe}] (**11** and **12**) (eq 1).



Two single resonances were observed in the ³¹P{¹H} NMR spectrum of the reaction mixture at δ 79.62 (**11**) and 87.62 ppm (**12**, major isomer) indicative of the equivalent P nuclei in the two complexes. The ¹H NMR spectrum revealed triplets of hydride resonances at δ -43.54 (t, *J*_{P-H} = 13.3 Hz) (**11**) and -39.48 ppm (t, *J*_{P-H} = 13.8 Hz) (**12**). The resonances of the cyclopentadienyl protons of the ferrocene unit are observed as two singlets at δ 4.54 (5H) and 4.37 (2H) for **11** and 3.86 (5H) and 3.78 (2H) for **12**, indicating cyclometalation of the substituted ring in both compounds. The spectroscopic data, in combination with mass spectrometry and elemental analysis, all support characterization of complexes **11** and **12** as indicated in eq 1; in particular, the ¹H NMR spectrum indicates a square-pyramidal geometry at iridium with the hydrido ligand in the apical position. Similar structures were reported for benzene-based pincer complexes RhH(Cl)[2,6-(^tBu₂PCH₂)₂C₆H₃]⁸ and IrH(Cl)[2,6-(^tBu₂PCH₂)₂-4-(NO₂)C₆H₂].⁹

The assignment of the isomeric complexes to the compounds with *endo*- (**11**) and *exo*-H (**12**) configuration is based on the NOE experiment and on CO stereoselective addition to **11** and **12** (vide infra). The hydride resonance of the major isomer shows apparent communication with the signal of the *tert*-butyl groups at δ 1.99 ppm and a lack of communication with the

(6) (a) Only ruthenocene-based chloro-hydrido complexes IrH(Cl)-[^t-Bu₂P,C,P^{Ru}] (*H-endo* and *H-exo* isomers) were briefly mentioned earlier, see: Koridze, A. A.; Sheloumov, A. M.; Kuklin, S. A.; Lagunova, V. Yu.; Petukhova, I. I.; Petrovskii, P. V. *Russ. Chem. Bull., Int. Ed.* **2003**, 52, 516–517. (b) Koridze, A. A. Alkane and alkane group dehydrogenation with organometallic catalysts. U.S. Patent, US 6,909,009, August 8, 2005.

(7) (a) Koridze, A. A.; Kuklin, S. A.; Sheloumov, A. M.; Dolgushin, F. M.; Lagunova, V. Yu.; Petukhova, I. I.; Ezernitskaya, M. G.; Peregodov, A. S.; Petrovskii, P. V.; Vorontsov, E. V.; Baya, M.; Poli, R. *Organometallics* **2004**, 23, 4585–4593. (b) Koridze, A. A.; Kuklin, S. A.; Sheloumov, A. M.; Kondrashov, M. V.; Dolgushin, F. M.; Peregodov, A. S.; Petrovskii, P. V. *Russ. Chem. Bull., Int. Ed.* **2003**, 52, 2754–2756. (c) Koridze, A. A.; Kuklin, S. A.; Sheloumov, A. M.; Kondrashov, M. V.; Dolgushin, F. M.; Ezernitskaya, M. G.; Petrovskii, P. V.; Vorontsov, E. V. *Russ. Chem. Bull., Int. Ed.* **2003**, 52, 2757–2759.

(8) (a) Moulton, C. J.; Shaw, B. L. *J. Chem. Soc., Dalton Trans.* **1976**, 1020–1024. (b) Nemeh, J. C.; Jensen, C.; Binamina-Soriaga, E.; Kaska, W. S. *Organometallics* **1983**, 2, 1442–1447.

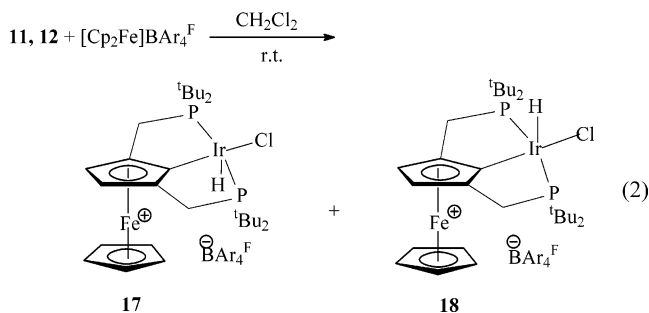
(9) Grimm, J. C.; Nachtigal, C.; Mack, H.-G.; Kaska, W. C.; Mayer, H. A. *Inorg. Chem. Commun.* **2000**, 3, 511–514.

unsubstituted cyclopentadienyl ring; the C_5H_5 ring shows a NOE to one pair of CH protons of the methylene groups (δ 2.87 ppm), indicating that they have the *endo*-arrangement. For the minor isomer, there is evidence for spacial proximity of the hydrido ligand to the C_5H_5 ring and to the protons of the *tert*-butyl groups at δ 1.53 ppm.

Cyclometalation of the ruthenocene diphosphine [$t\text{-BuP,C,H,P}^{\text{Ru}}$] (**13**), generated from 1,3-bis(hydroxymethyl)ruthenocene and HP^tBu_2 , by $[\text{Ir}(\text{COE})_2\text{Cl}]_2$ occurs analogously to give two chloro-hydrido complexes, *H-endo*- (**14**) and *H-exo*- $\text{IrH}(\text{Cl})$ -[$t\text{-BuP,C,P}^{\text{Ru}}$] (**15**).^{6a}

The ratio of **11** and **12**, as well as that of **14** and **15**, in the resulting mixtures depends on the temperature and duration of thermal reaction. *H-exo* isomers **12** and **15** are the major products of the thermal reaction in refluxing toluene. However, we observed that complex **11** is the predominant product formed at the early stage of the reaction (C_6D_6 as a solvent, room temperature, 1 h, NMR tube). Thus, the product having the *endo*-H configuration is initially formed and further rearranges into the *exo*-isomer. Cyclometalation of diphosphine **10** in refluxing toluene for 6 h gives a mixture of **11** and **12** in a ratio of ca. 2:5. However, when this mixture was heated in refluxing cyclooctane (151 °C), complex **11** completely converted into isomer **12** without any sign of product decomposition. Similar rearrangement of related rhodium complex *H-endo*- $\text{RhH}(\text{Cl})$ -[$t\text{-BuP,C,P}^{\text{Rh}}$] into the *exo*-isomer was observed recently by J. M. Brown, G. van Koten, et al.¹⁰

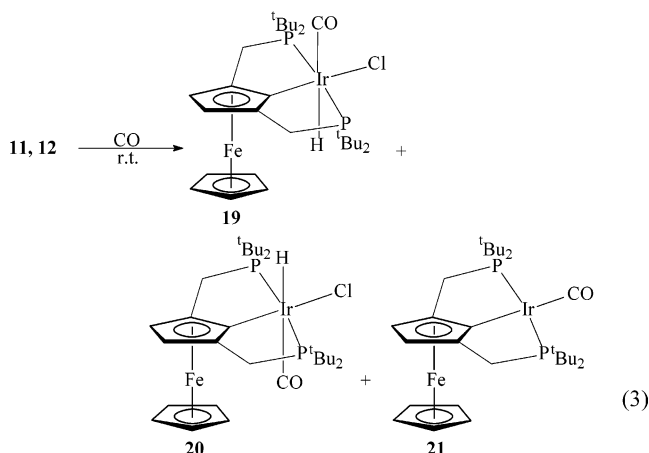
1.2. Chemical Oxidation of 11 and 12. Recently we reported chemical and electrochemical oxidation of chloropalladium complex **8b** centered on the iron atom.^{7a} Ferrocenium-based complex $[\text{PdCl}][t\text{-BuP,C,P}^{\text{Fe}}]\text{PF}_6$ (**16**) isolated from the reaction of **8b** with $[\text{Cp}_2\text{Fe}]\text{PF}_6$ was characterized by ^1H and $^{31}\text{P}\{^1\text{H}\}$ NMR spectra and elemental analysis. Now we found that iridium chloro-hydrido complexes **11** and **12** (a mixture of **11** and **12** in a ratio of ca. 2:5) react with $[\text{Cp}_2\text{Fe}]\text{BAR}_4^{\text{F}}$ ($\text{Ar}^{\text{F}} = 3,5\text{-(CF}_3)_2\text{C}_6\text{H}_3$) to form paramagnetic complexes, $\{\text{H-endo-IrH}(\text{Cl})[t\text{-BuP,C,P}^{\text{Fe}}]\}\text{BAR}_4^{\text{F}}$ (**17**) and $\{\text{H-exo-IrH}(\text{Cl})[t\text{-BuP,C,P}^{\text{Fe}}]\}\text{BAR}_4^{\text{F}}$ (**18**), respectively (eq 2).



In the ^1H NMR spectrum of the resulting mixture, the major isomer **18** reveals methyl protons of the *tert*-butyl groups at δ -6.76 and 7.33 ppm; the methylene group protons of $\text{CH}_2\text{P}^t\text{Bu}_2$ appear at δ -126.08 (very broad) and -63.33 ppm (broad). For the minor isomer **17**, the corresponding resonances are observed at δ -5.73 and 7.57 ppm and -101.26 and -68.83 ppm. Remarkably, the resonances of the phosphorus nuclei in the $^{31}\text{P}\{^1\text{H}\}$ NMR spectrum, δ 49.11 (**17**) and 54.39 ppm (**18**), are sharp, as was the case for paramagnetic complex **16**.

1.3. Reactions of Chloro-Hydrido Complexes 11 and 12 with CO. X-ray Crystallography of *H-exo*- $\text{IrH}(\text{Cl})(\text{CO})$ -[$t\text{-BuP,C,P}^{\text{Fe}}$] (**20**). Stereochemical assignment of isomeric

complexes **11** and **12** based on the spectroscopic data was confirmed by the stereospecific reaction of **11** and **12** with CO and the X-ray diffraction study of one of the CO adducts. Thus, both **11** and **12** smoothly react with CO, affording octahedral 18-electron complexes *H-endo*- (**19**) and *H-exo*- $\text{IrH}(\text{Cl})(\text{CO})$ -[$t\text{-BuP,C,P}^{\text{Fe}}$] (**20**), respectively (eq 3).



Complex **19**, as well as its precursor **11** in the initial mixture, is the minor product of the reaction. Besides complexes **19** and **20**, the reaction mixture contains a small amount of complex $\text{Ir}(\text{CO})[t\text{-BuP,C,P}^{\text{Fe}}]$ (**21**); this was identified by comparison of the spectral data with those for the authentic sample, obtained in another reaction and fully characterized (vide infra).

Complexes **19** and **20** were identified on the basis of IR and ^1H and $^{31}\text{P}\{^1\text{H}\}$ NMR spectra. The major isomer **20** was isolated from the mixture in analytically pure form and was fully characterized by a single-crystal X-ray diffraction study. A single resonance was observed for two equivalent phosphorus nuclei in the $^{31}\text{P}\{^1\text{H}\}$ NMR spectrum, at δ 71.28 (**19**) and 66.72 ppm (**20**). In the ^1H NMR spectrum, resonances of the hydrido ligands of these complexes are observed at δ -6.59 (t, $J_{\text{P-H}} = 14.3$ Hz) (**19**) and -8.62 (t, $J_{\text{P-H}} = 15.3$ Hz) (**20**). The CO stretch for **19** and **20** is observed at 2025 and 1997 cm^{-1} , respectively. (The difference in the ν_{CO} frequencies of complexes **19** and **20** may mainly originate from the different sterical environment of the CO ligands; thus, the CO ligand in complex **19** should be subject to steric congestion by the axial *tert*-butyl groups at the P atoms.) For the related benzene-based complex $\text{IrH}(\text{Cl})(\text{CO})[2,6\text{-(}^t\text{Bu}_2\text{PCH}_2)_2\text{C}_6\text{H}_3]$ ^{8a} with the same configuration at the Ir center, the resonance of the hydrido ligand appears at δ -7.6 ppm ($J_{\text{P-H}} = 15$ Hz) in the ^1H NMR spectrum and the CO stretch was observed at 1985 cm^{-1} in the IR spectrum. For pincer complex $\text{IrH}(\text{Cl})(\text{CO})[2,6\text{-(}^i\text{Pr}_2\text{PCH}_2)_2\text{C}_6\text{H}_3]$,¹¹ which has a different ligand arrangement at the Ir atom, where H and Cl ligands are *trans* to each other, the resonance of the hydrido ligand was observed in a substantially stronger field, at δ -18.3 ppm ($J_{\text{P-H}} = 11.6$ Hz).

Orange prismatic crystals of **20** were obtained by slow evaporation from an *n*-hexane-benzene solution. The molecular structure of **20** is shown in Figure 1; the view projected along the substituted cyclopentadienyl ring is illustrated in Figure 2.

The geometry around Ir(1) can be described as a distorted octahedron with CO and H ligands in the *endo* and *exo* positions, respectively, i.e., as expected on the basis of stereochemistry proposed for the precursor **12** and stereoselective CO addition to the empty coordination site. The distortion originates from

(10) Farrington, E. J.; Viviente, E. M.; Williams, B. S.; van Koten, G.; Brown, J. M. *Chem. Commun.* **2002**, 308-309.

(11) Rybtchinski, B.; Vigalok, A.; Ben-David, Y.; Milstein, D. *J. Am. Chem. Soc.* **1996**, *118*, 12406-12415.

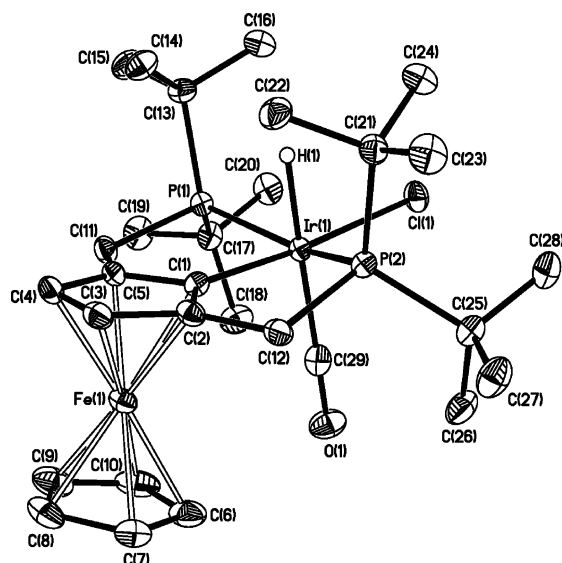


Figure 1. ORTEP presentation of the molecular structure with numbering scheme for complex **20**, with thermal ellipsoids drawn at the 50% probability level (the hydrogen atoms, except for hydride ligand H(1), have been omitted for clarity). Selected bond lengths (Å) and angles (deg): Ir1–C1 2.015(3), Ir1–P1 2.3645(7), Ir1–P2 2.3737(8), Ir1–H1 1.56(4), Ir1–C11 2.4923(7), Ir1–C29 1.934(3); P1–Ir–P2 152.99(2), C29–Ir1–C1 93.8(1), C1–Ir1–C11 175.15(8), C1–Ir1–H1 86(2), C1–C2–C12 118.8(3), C1–C5–C11 119.5(3).

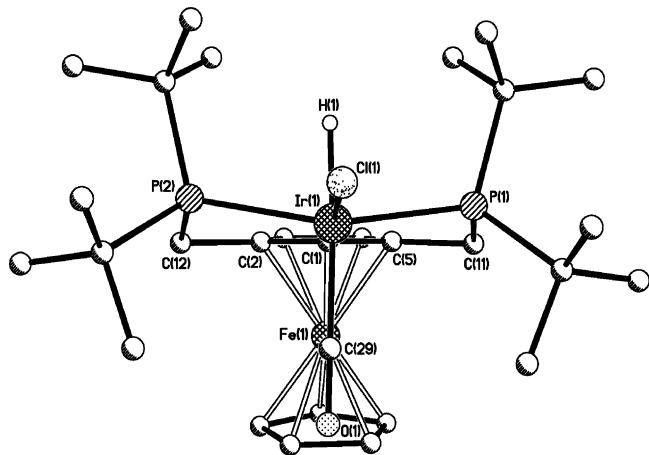


Figure 2. Molecular structure of **20**; view projected along the substituted cyclopentadienyl ring (the hydrogen atoms, except for hydride ligand H(1), have been omitted for clarity).

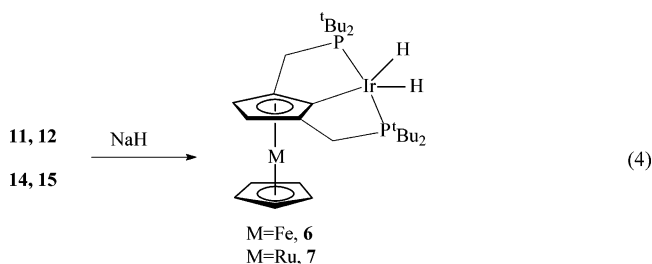
the geometry of the P,C,P ligand. The P(1)–Ir(1)–P(2) angle (152.99(2)°) is markedly less than those observed for other ferrocene-based P,C,P pincer complexes: *cis*-RhCl₂(CO)-[i-PrP,C,P^{Fe}]¹² (161.92(4)°), PdCl[i-PrP,C,P^{Fe}]⁷ (160.39(6)°), PdCl[t-BuP,C,P^{Fe}]⁷ (157.57(4)°), and Pd(BH₄)[t-BuP,C,P^{Fe}]⁷ (160.72(3)°). The Ir(1)–C(1) bond distance of 2.015(3) Å is comparable with those observed for IrH₂[2,6-(^tBu₂PCH₂)₂C₆H₃]^{4b} (2.12(1) Å), IrH(OH)[2,6-(^tBu₂PCH₂)₂C₆H₃]¹³ (2.012(2) Å), and Ir(CO)[2,6-(^tBu₂PCH₂)₂C₆H₃]¹⁴ (2.102(8) Å). The Ir–P dis-

tances (average mean 2.3689(7) Å) in complex **20** are somewhat longer in comparison with those for benzene-based P,C,P iridium pincer complexes (2.304(2)–2.3124(12) Å).

As for other ferrocene-based P,C,P pincer complexes, the bond angles for **20** at C(2) and C(5) in the fused metallacycles (C(1)–C(2)–C(12) (118.8(3)°) and C(1)–C(5)–C(11) (119.5(3)°) are smaller than the standard value of 126° for the cyclopentadienyl ring. The chelated metal atom in **20** is lifted above the cyclopentadienyl plane by 0.358 Å. The cyclopentadienyl rings deviate from parallel by 6.0° and have a staggered conformation (relative orientation angle is 32.5°). Remarkably, the staggered conformation of the cyclopentadienyl rings was found only in the ferrocene-based pincer complexes having the octahedral arrangement at the chelated metal atom with the CO ligand in the *endo*-position relative to iron.¹² This might be due to steric contacts between the CO ligand and the unsubstituted ring, since in other cases, for example, for complexes **8a,b** and **9b**, only the eclipsed conformation is observed. The substituted cyclopentadienyl ring in **20** is not perfectly planar, the carbon atom C(1) deviates from the C(2)C(3)C(4)C(5) plane by 0.05 Å in the direction opposite the iron atom; the folding the ring across C(2)···C(5) is 3.5°.

The overall stereochemistry of the ^tBu₂PCH₂ groups in **20** is very similar to that of other ferrocene-based pincer complexes.⁷ As may be seen from Figure 2, the P(1) and P(2) atoms are located on the same side of the substituted cyclopentadienyl ring (opposite the iron atom), in contrast to the benzene-based bis(phosphine) pincer complexes, where they are situated at the opposite sides of the cyclometalated ring. As a consequence, in **20** two ^tBu groups are axial and strongly shield the *exo*-position at the chelated metal atom, whereas two other ^tBu groups are pseudoequatorial. Evidently, this arrangement of the axial ^tBu groups should prevent the addition of bulky, not rodlike ligands (e.g., tertiary phosphines) and substrates to the position *exo* to the chelated metal atom in ferrocene-based systems.

2. Formation and Reactivity of Hydrido Complexes IrH_n[^t-Bu_nP,C,P^M] (M = Fe, *n* = 2, 4; Ru, *n* = 2).
2.1. Formation of Metallocene-Based Hydrido Complexes of Iridium. Reaction of chloro-hydrido complexes **11**, **12** and **14**, **15** with excess NaH in refluxing cyclooctane gave the corresponding dihydrido iridium complexes **6** and **7** (eq 4).



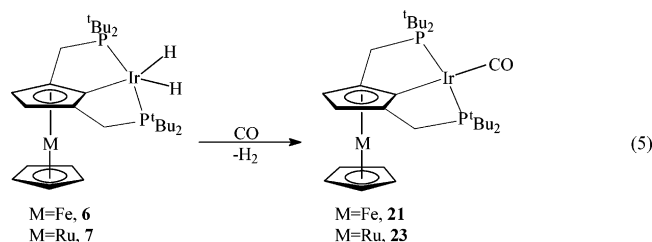
Complexes **6** and **7** are air sensitive and were characterized by NMR spectroscopy and by transformation into corresponding carbonyl derivatives Ir(CO)[^t-Bu_nP,C,P^M] (M = Fe, **21**; M = Ru, **23**) when reacting with CO. Dihydride **6** adds hydrogen to give tetrahydrido complex IrH₄[^t-Bu_nP,C,P^{Fe}] (**22**). Tetrahydride **22** is not stable under reduced pressure at room temperature and reversibly loses hydrogen to give dihydride **6**. Complex **22** is highly fluxional owing to migration of hydrido ligands. The results of the study of the stereochemical nonrigidity of **22** will be published separately.

2.2. Reaction of Dihydrido Iridium Complexes with CO and CN^tBu. Chemical Oxidation of Ir(CO)[^t-Bu_nP,C,P^{Fe}] (21**).** Complexes **6** and **7** react smoothly with carbon monoxide at

(12) Koridze, A. A.; Sheloumov, A. M.; Kuklin, S. A.; Lagunova, V. Yu.; Petukhova, I. I.; Dolgushin, F. M.; Ezernitskaya, M. G.; Petrovskii, P. V.; Macharashvili, A. A.; Chedia, R. V. *Russ. Chem. Bull., Int. Ed.* **2002**, *51*, 1077–1078.

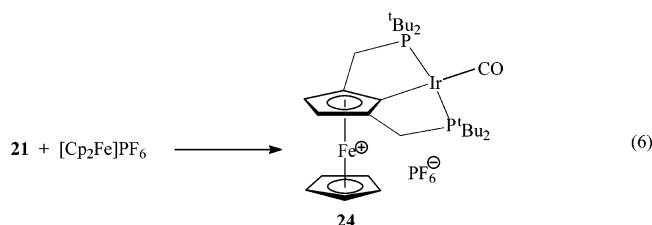
(13) Morales-Morales, D.; Lee, D. W.; Wang, Z.; Jensen, C. M. *Organometallics* **2001**, *20*, 1144–1147.

ambient temperature with displacement of H₂, giving the corresponding carbonyl complexes Ir(CO)[t-BuP,C,P^M] (M = Fe, **21**; M = Ru, **23**) (eq 5).

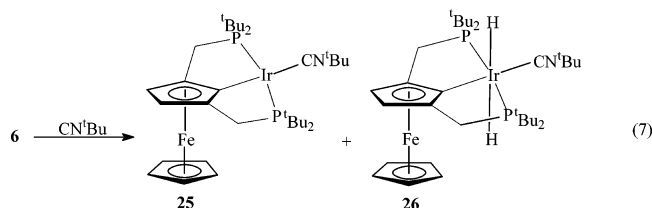


Compounds **21** and **23** are air-stable crystalline solids. They were characterized by IR and NMR spectroscopy and by elemental analysis. The structure of complex **21** was confirmed by X-ray diffraction (vide infra).

Complex **21** reacts with the equivalent amount of [Cp₂Fe]-PF₆ in methylene chloride to form ferrocenium-based pincer complex {Ir(CO)[t-BuP,C,P^{Fe}]}PF₆ (**24**) (eq 6). Paramagnetic complex **24** was characterized by ¹H and ³¹P{¹H} NMR spectra. In the ¹H NMR spectrum, the methyl protons of the *tert*-butyl groups are observed at δ -8.22 and 6.46 ppm; the methylene group protons of CH₂P^tBu₂ appear at δ -115.20 (very broad) and -43.57 ppm (broad); the protons of the unsubstituted and substituted cyclopentadienyl rings appear at δ 20.22 (broad) and 32.10 ppm (very broad). In the ³¹P{¹H} spectrum two equivalent phosphorus atoms of the pincer ligand are observed as a singlet at δ 40.26 ppm.

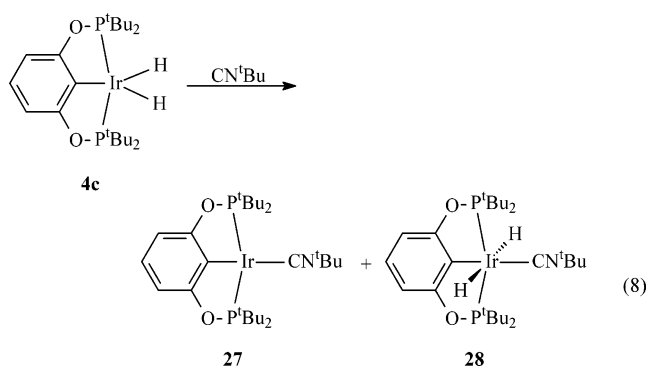


In contrast to the reaction with CO, complex **6** reacts with CN^tBu, giving two pincer compounds, the product of substitution, Ir(CN^tBu)[t-BuP,C,P^{Fe}] (**25**), and the product of addition, IrH₂(CN^tBu)[t-BuP,C,P^{Fe}] (**26**), in a ratio of ~3:1 (eq 7). In the hydride region of the ¹H NMR spectrum of **26**, there are two resonances, at δ -14.01 (dt, J_{H-H} = 2.5 Hz, J_{P-H} = 16.4 Hz) and -11.37 ppm (dt, J_{H-H} = 2.5 Hz, J_{P-H} = 11.8 Hz).



It is noteworthy that the known^{4e} bis-phosphinite complex IrH₂[2,6-(^tBu₂PO)₂C₆H₃] (**4c**) reacts with CN^tBu analogously to **6**, giving complexes Ir(CN^tBu)[2,6-(^tBu₂PO)₂C₆H₃] (**27**) and IrH₂(CN^tBu)[2,6-(^tBu₂PO)₂C₆H₃] (**28**) in a ratio of ~5:1 (eq 8). In the ¹H NMR spectrum of **28**, a single resonance is observed at δ -10.82 (t, J_{P-H} = 16.8 Hz) resulting from two equivalent hydrido ligands.

3. Electronic Properties of the Ir[P,C,P] Fragments. 3.1. ν_{CO} Stretching Frequencies. Carbonyl stretching frequency is a sensitive tool for the evaluation of electronic properties of the corresponding metal centers with their ancillary ligands



bound to the carbonyl group.¹⁵ It is of interest to compare electronic effects of different Ir[P,C,P] fragments revealed from ν_{CO} stretching of carbonyl complexes. Carbonyl stretching frequencies of the metallocene-based pincer complexes are listed in Table 1; for comparison the data for related benzene-based complexes^{4e,16} are also included.

The ν_{CO} stretching frequencies measured in CH₂Cl₂ solution for ferrocene- (**21**) (1904 cm⁻¹) and ruthenocene-based (**23**) (1905 cm⁻¹) complexes are very similar, whereas the stretching frequency for **24** (1951 cm⁻¹) is strongly shifted as compared to those for **21** and **23**, indicating significant electron-withdrawing ability of the oxidized iron center in {Ir[t-BuP,C,P^{Fe}]}⁺.

The ν_{CO} stretching frequencies for metallocene-based complexes Ir(CO)[t-BuP,C,P^M] (M = Fe, **21**; M = Ru, **23**) (1926 cm⁻¹) are very close to that for the benzene-based analogue Ir(CO)[2,6-(^tBu₂PCH₂)₂C₆H₃] (**29**) (1927.7 cm⁻¹) in hydrocarbon solution; however, the bis(phosphinite) complex Ir(CO)-[2,6-(^tBu₂PO)₂C₆H₃] (**30**) has a ν_{CO} stretching frequency at a significantly higher value (23 cm⁻¹).

Thus, comparing the ν_{CO} stretching of carbonyl adducts, we may conclude that the iridium centers in metallocene-based Ir[t-BuP,C,P^M] and benzene-based bis(phosphine) Ir[2,6-(^tBu₂PCH₂)₂C₆H₃] fragments are more electron-rich than that in the benzene-based bis(phosphinite) Ir[2,6-(^tBu₂PO)₂C₆H₃] fragment.

3.2. Near-Infrared Spectra. Electronic properties of the bridging ligand in binuclear pincer complexes can be estimated not only from ν(CO) frequencies for carbonyl complexes but also from the degree of intramolecular charge transfer between two metal centers in cationic complexes.

There are numerous data in the literature concerning intramolecular charge transfer in binuclear complexes, where two metallic centers are connected via an organic ligand capable of conducting electron density (for example, a chain of sp-hybridized atoms). It is known for this type of compound that one-electron oxidation of one metallic center yields a complex for which in the NIR spectrum a broad intense band appears associated with intervalence charge transfer (so-called IT band) from one metallic center to the other via bridging ligand. The intensity of this band is very sensitive to the degree of interaction between metallic centers of different valence.

The NIR spectra were measured for the neutral complex Ir(CO)[t-BuP,C,P^{Fe}] (**21**) and the cationic complex {Ir(CO)-[t-BuP,C,P^{Fe}]}PF₆ (**24**) in a CH₂Cl₂ solution. While the neutral complex **21** shows no absorption in the near-IR region, the NIR spectrum of the cationic complex **24** has two broad, intense (ε

(14) Morales-Morales, D.; Redon, R.; Wang, Z.; Lee, D. W.; Yung, C.; Magnuson, K.; Jensen, C. M. *Can. J. Chem.* **2001**, *79*, 823–829.

(15) Crabtree, R. H. *The Organometallic Chemistry of the Transition Metals*, 3rd ed.; John Wiley & Sons: New York, 2001; pp 46–47.

(16) Krogh-Jespersen, K.; Czerw, M.; Zhu, K.; Singh, B.; Kanzelberger, M.; Darji, N.; Achord, P. D.; Renkama, K. B.; Goldman, A. S. *J. Am. Chem. Soc.* **2002**, *124*, 10797–10809.

Table 1. Carbonyl ν_{CO} Stretching Frequencies for Pincer Complexes

compound	ν_{CO} (cm^{-1})	
	hydrocarbon solution	CH_2Cl_2 solution
$\text{Ir}(\text{CO})[\text{t-BuP,C,P}^{\text{Fe}}]$ (21)	1926 ^a	1904
$\text{Ir}(\text{CO})[\text{t-BuP,C,P}^{\text{Ru}}]$ (23)	1926 ^a	1905
$\{\text{Ir}(\text{CO})[\text{t-BuP,C,P}^{\text{Fe}}]\}\text{PF}_6$ (24)		1951
$\text{Ir}(\text{CO})[2,6\text{-}(\text{t-Bu}_2\text{PCH}_2)_2\text{C}_6\text{H}_3]$ (29)	1927.7 ^b	
$\text{Ir}(\text{CO})[2,6\text{-}(\text{t-Bu}_2\text{PO})_2\text{C}_6\text{H}_3]$ (30)	1949 ^c	

^a Hexane solution. ^b Cyclooctane solution, ref 16. ^c Pentane solution, ref 4e.

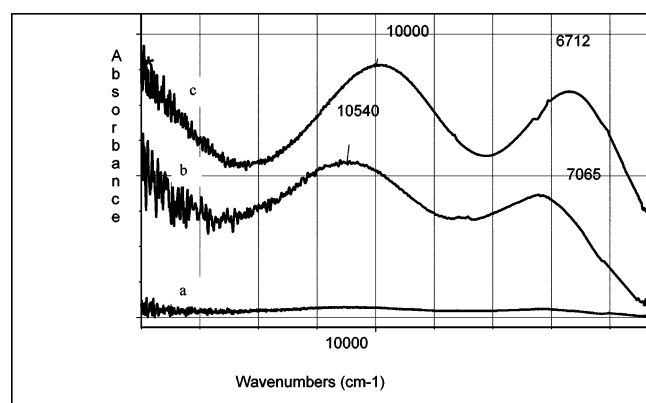


Figure 3. NIR spectra of complexes **21** and **24**. (a) NIR spectrum of complex **21** in CH_2Cl_2 ; (b) NIR spectrum of complex **24** in acetone; (c) NIR spectrum of complex **24** in CH_2Cl_2 .

about $50\,000\text{ mol}^{-1}\text{ cm}^{-1}$ absorption bands with maxima at about $10\,000$ and 7000 cm^{-1} (Figure 3), which are assigned to intervalence transfer (IT bands) and are, therefore, indicative of electron density delocalization between two metallic centers. These bands are solvatochromic, but the solvent dependence of band position is not large: the hypsochromic shift on going from methylene chloride to acetone is 540 and 353 cm^{-1} , respectively.

Using the Hush methodology,¹⁷ the interaction parameter α^2 , indicating the degree of charge delocalization between two metallic centers of different valence, was estimated by the formula

$$\alpha^2 = (4.2 \times 10^{-4}) \epsilon_{\text{max}} \Delta\nu_{1/2} / \nu_{\text{max}} d^2$$

where ν_{max} is the position of the IT band in cm^{-1} , ϵ_{max} is the extinction, $\Delta\nu_{1/2}$ is the band half-width, and d is the distance between two metallic centers.

For most mixed-valence complexes studied, the charge transfer between two metallic centers occurs via a linear bridging ligand and the d value coincides with the X-ray metal–metal distance. For iron(II) ferrocenylacetylide diphosphine complexes¹⁸ the direct distance between two Fe atoms was taken as an estimate. We believe that if charge transfer occurs via the ligand, it seems more reasonable to take the sum of the Fe–C1 and C1–Ir distances (4.129 Å) as a d value. However, the use of the direct distance between two metallic centers (3.767 Å) does not much influence the α^2 value.

The parameters of the IT band for complex **24** are presented in Table 2.

Table 2. Parameters of the IT Bands in the NIR Spectra of Complex 24

complex/solvent	ν (cm^{-1})	λ (nm)	ϵ ($\text{mol}^{-1}\text{ cm}^{-1}$)	$\Delta\nu_{1/2}$ (cm^{-1})	α^2
24 in CH_2Cl_2	10 000	1000	53 770	2769	0.37
	6712	1490	49 540	2997	0.54
24 in acetone	10 540	949	23 457	2446	0.13
	7065	1415	27 740	2035	0.20

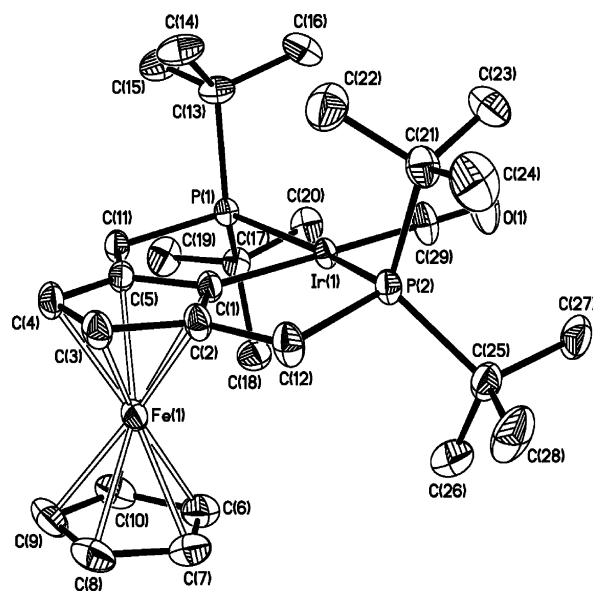


Figure 4. ORTEP presentation of the molecular structure with numbering scheme for complex **21**, with thermal ellipsoids drawn at the 30% probability level (hydrogen atoms have been omitted for clarity). Selected bond lengths (Å) and angles (deg): Ir1–C1 2.025(3), Ir1–P1 2.302(1), Ir1–P2 2.310(1), Ir1–C29 1.857(3), P1–C11 1.866(3), P2–C12 1.870(3); P1–Ir1–P2 157.91(3), C1–Ir1–P1 80.3(1), C1–Ir1–P2 79.8(1), C1–C5–C11 118.9(3), C1–C2–C12 118.1(3), C29–Ir1–C1 179.3(2), O1–C29–Ir1 179.5(4).

According to these parameters, in complex **24** there is a high degree of intramolecular charge transfer from the Fe to Ir atom via the P,C,P ligand, but the charge separation between two metallic centers still exists. This is in accord with a high value of CO stretching vibrations in the IR spectrum indicative of electron-withdrawing ability of the ferrocenium moiety; however, the α^2 parameter provides an estimation of the degree of intermetallic interaction. In addition, the NIR approach is useful for cationic complexes having no carbonyl ligands. The α^2 values obtained for complex **24** are about 1 order of magnitude higher than those for other mixed-valence complexes containing the ferrocenium moiety.¹⁸

That means that the ability of the $\text{R}^{\text{P,C,P}}\text{M}$ ligand to transfer electronic density from one metal center to the other allows fine-tuning of electronic density at the Ir atom by introducing substituents into the metallocenyl moiety.

3.3. X-ray Diffraction Study. Further information about electronic properties of the $\text{Ir}[\text{P,C,P}]$ fragments can be extracted from the X-ray diffraction study of iridium carbonyl complexes by comparison of the Ir–CO distances. The X-ray crystal structures of the ferrocene-based complex $\text{Ir}(\text{CO})[\text{t-BuP,C,P}^{\text{Fe}}]$ (**21**) and benzene-based bis(phosphinite) complex $\text{Ir}(\text{CO})[2,6\text{-}(\text{t-Bu}_2\text{PO})_2\text{C}_6\text{H}_3]$ ^{4e} (**30**) were determined in the present study. The complex $\text{Ir}(\text{CO})[2,6\text{-}(\text{t-Bu}_2\text{PCH}_2)_2\text{C}_6\text{H}_3]$ (**29**) was characterized earlier by X-ray crystallography.¹⁴

The molecular structures of complexes **21** and **30** are presented in Figure 4 and Figure 5. The Ir(1)–C(29)–O(1) angle is equal to $179.5(4)^\circ$ in complex **21**, and the P(1)–Ir(1)–P(2) angle ($157.91(3)^\circ$) is in the range reported for other ferrocene-

(17) (a) Hush, N. S. *Coord. Chem. Rev.* **1985**, *64*, 135–157. (b) Hush, N. S. *Progr. Inorg. Chem.* **1967**, *8*, 391–444.

(18) Sato, M.; Hayashi, Y.; Kumakura, S.; Shimuzi, N.; Katada, M.; Kawata, S. *Organometallics* **1996**, *15*, 721–728.

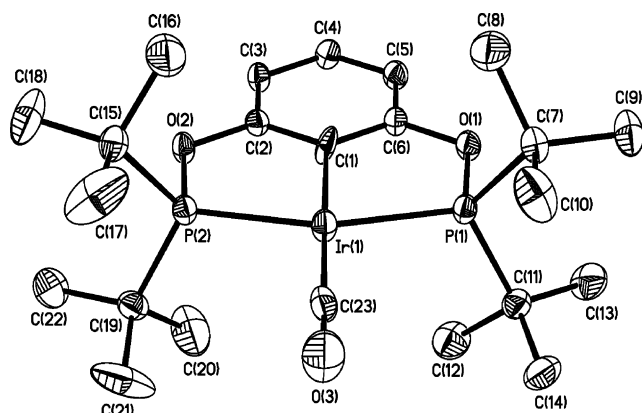


Figure 5. ORTEP presentation of the molecular structure with numbering scheme for complex **30**, with thermal ellipsoids drawn at the 50% probability level (hydrogen atoms have been omitted for clarity). Selected bond lengths (Å) and angles (deg.): Ir1–C1 2.046(3), Ir1–P1 2.2825(8), Ir1–P2 2.2822(9), Ir1–C23 1.880(4); P1–Ir1–P2 157.55(3), O1–C6–C1 117.7(3), O2–C2–C1 118.2(3).

based pincer complexes.⁷ The C(1)–Ir(1) distance is 2.025(3) Å; the chelated iridium atom deviates from the plane of the cyclopentadienyl ring, being 0.159 Å above the ring. The cyclopentadienyl rings in **21** deviate from parallel by 4.0°. The substituted cyclopentadienyl ring in **21** is not perfectly planar; the carbon atom C(1) deviates from the C(2)C(3)C(4)C(5) plane by 0.04 Å in the direction opposite the iron atom (folding across C(2)···C(5) being 2.6°).

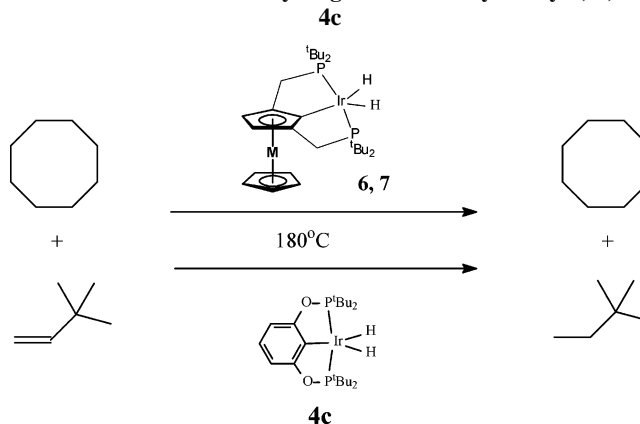
The Ir–CO distance of 1.857(3) Å in ferrocene-based complex **21** is somewhat shorter than in benzene-based bis(phosphinite) complex **30**, 1.880(4) Å. This is in agreement with the ν_{CO} stretching for complexes **21** and **30**, since back-donation of electron density from the Ir[^t-BuP,C,P^{Fe}] fragment to the CO ligand is expected to be larger than that from the Ir[2,6-(^tBu₂PO)₂C₆H₃] fragment. However, the correlation of ν_{CO} and Ir–CO distances is not so straightforward when we compare the data for benzene-based bis(phosphine) pincer complex Ir(CO)[2,6-(^tBu₂PCH₂)₂C₆H₃] (**29**). According to the X-ray diffraction study,¹⁴ for two crystallographic isomers, the Ir–CO distances are 1.873(10) and 1.852(12) Å. Notably, the values of the P(1)–Ir–P(2) angle for these isomers in **29** (164.510(8)° and 163.080(9)°) are markedly larger than those in complexes **21** (157.91(3)°) and **30** (157.55(3)°).

Thus, the CO stretching is more sensitive for the evaluation of electronic effects than the Ir–CO distances. According to the ν_{CO} of carbonyl adducts of Ir[P,C,P] fragments, the electron density on the iridium atom increases in the following order: {Ir[^t-BuP,C,P^{Fe}]}⁺ < Ir[2,6-(^tBu₂PO)₂C₆H₃] < Ir[2,6-(^tBu₂PCH₂)₂C₆H₃] ≤ Ir[^t-BuP,C,P^{Ru}] ≈ Ir[^t-BuP,C,P^{Fe}]. Obviously, alkane C–H bond oxidative addition to the iridium atom may be expected to be the most favored for the metallocene-based systems.

At the same time, the comparison of the X-ray data for three types of iridium pincer complexes revealed a marked difference in the values of the P(1)–Ir–P(2) angles, which for complexes **21**, **30**, and **29** are equal to 157.91(3)°, 157.55(3)°, and 164.510(8)°, 163.080(9)° (two isomers), respectively. These data presume that the iridium center should be sterically more accessible for the substrate in Ir[^t-BuP,C,P^{Fe}] and Ir[2,6-(^tBu₂PO)₂C₆H₃] than in Ir[2,6-(^tBu₂PCH₂)₂C₆H₃].

On the basis of the above discussions it is interesting to see if the above-mentioned electronic and steric peculiarities of our metallocene-based iridium systems would result in a greater

Scheme 1. Transfer Dehydrogenation Catalyzed by **6**, **7**, or **4c**



catalytic activity in alkane dehydrogenation in comparison to known benzene-based pincer iridium complexes.

4. Catalytic Activity of Complexes IrH₂[^t-BuP,C,P^M] (M = Fe, **6; M = Ru, **7**).** Recently Brookhart et al.^{4d} have shown that bis(phosphinite) iridium pincer complexes **4a–f** are more active catalysts for cyclooctane transfer dehydrogenation in the presence of *tert*-butylethylene than their bis(phosphine) analogues. Thus, in a series of experiments, reaction of COA, TBE, and **4a–f** gave 1484–2070 turnover numbers (TONs) after 40 h at 200 °C, whereas 227 TONs were obtained under similar conditions with **1a** as a catalyst. As follows from ν_{CO} frequencies of the respective carbonyl adducts, the iridium center in bis(phosphinite) complexes is less electron rich than in their bis(phosphine) analogues. The Hammett σ constants for substituents X in **4a–f** increase with increasing electron deficiency of the catalytic center and correlate with initial TONs of the catalyst. However, in the course of further reaction, this correlation does not hold, and the TON for the catalyst **4a** becomes close to that for **4e,f**.

Goldman et al.^{4h} studied iridium pincer complexes with a *p*-methoxy substituent in the benzene ring, IrH₂[^t-BuP,C,P-OMe] (**1b**) and IrH₂[ⁱ-PrP,C,P-OMe] (**2b**), by experimental and computational methods. The calculations showed that thermodynamic and kinetic properties are equally affected by the presence of the *p*-methoxy substituent and by the substitution of the ligand methylene groups bound to phosphorus with the oxygen atoms (to form PO,C,OP) even though these substitutions affect ν_{CO} values in the opposite directions.

We tested the catalytic activity of metallocene-based iridium hydrido complexes **6** and **7** in COA dehydrogenation in the presence of TBE (Scheme 1). Complexes **6** and **7** were generated by the treatment of the corresponding chloro-hydrido complexes with NaH in COA. For the sake of comparison, the catalytic activity of known bis(phosphinite) complex **4c** generated similarly was also studied. When 1:1 (mol:mol) COA/TBE solutions of the catalysts were heated for 8 h in a 180 °C oil bath, TONs of 3300, 2571, and 1843 were obtained for **6**, **7**, and **4c**, respectively. No formation of 1,3-cyclooctadiene was observed under these conditions. Thus, metallocene-based complexes **6** and **7** exhibit unprecedented activity in the transfer dehydrogenation of cyclooctane, ferrocene-based complex **6** being significantly more active than the ruthenocene analogue **7**.

As was already mentioned,^{4d,h} there seems to be no simple general explanation of catalytic properties manifested by various iridium pincer complexes. Further experimental and computational studies are required, which will provide deeper understanding of this very important reaction. However, even now some observations deserve comments. First of all, the question

arises, what is the reason for the increased activity of complexes **6** and **7** in COA dehydrogenation and for such a significant difference in activity for “isostructural” complexes **6** and **7**.

The consideration of the relationship between steric factors and catalytic activity of our and known iridium pincer complexes indicates that steric availability of the iridium center for a substrate may be a factor of primary importance. Steric availability of the catalytic center is determined by the P–Ir–P angle value and by the bulkiness of the organyl groups at the phosphorus donor atoms.

The comparison of the values of P–Ir–P angles for carbonyl complexes, ferrocene-based complex **21** (157.91(3)°), and bis(phosphinite) complex **30** (157.55(3)°) shows that they are markedly smaller than those for bis(phosphine) complex **29** (164.510(8)° and 163.080(9)° for two isomers). Consequently, we may expect that the iridium atoms in complexes **6**, **7**, and **4c** are more available for substrate than that in complex **1a**, being in accord with a relatively low activity of the latter complex in comparison with bis(phosphinite) complexes **4a–f**.^{4d} Goldman et al.^{4h} also noted that while the introduction of a *p*-methoxy group into a benzene ring of the parent complex IrH₂[^t-BuP,C,P] only slightly facilitates catalysis, substitution of the *tert*-butyl groups at the P donor atoms for isopropyl groups has a much more favorable effect.

As for metallocene-based complexes **6** and **7** bearing the same *tert*-butyl groups at the phosphorus donor atoms, at first glance the difference in the availability of the iridium centers for substrate seems to be minimal. However, in metallocene-based complexes, in addition to two steric factors imposed by the value of the P–Ir–P angle and the bulkiness of organyl groups at the P donor atoms, there is a third steric factor caused by a close contact of the pseudoequatorial alkyl groups and the unsubstituted (nonmetalated) cyclopentadienyl ring of the metallocene framework. The different availability of the iridium atoms for substrate can be dictated by nonequal distances between the cyclopentadienyl rings in ferrocene and ruthenocene, 3.32 and 3.682 Å, respectively.^{19,20} In metallocene-based pincer complexes, the cyclopentadienyl rings can deviate from being parallel, presumably due to a close contact between the unsubstituted ring and pseudoequatorial alkyl groups at the phosphorus atoms. Thus, the tilting angle of the cyclopentadienyl rings is 4.5° for PdCl[^t-BuP,C,P^{Fe}]⁷ (**8b**), whereas it is only 2.6° for PdCl[^t-BuP,C,P^{Ru}]²¹ (**31**). As for the P–Pd–P angle, it is 157.57(4)° for **8b** and 157.94(3)° for **31**.

In ferrocene- and ruthenocene-based pincer complexes, the above-mentioned steric contacts might also cause nonequal deviation of the chelated metal atom from the plane of the substituted cyclopentadienyl ring. For instance, the deviations of the Pd atom from the cyclopentadienyl ring plane are 0.069 and 0.007 Å for **8b** and **31**, respectively. For Pd(BH₄)-[^t-BuP,C,P^{Fe}]⁷ (**9b**), modeling an earlier stage of alkane (methane) oxidative addition to the catalytic species Ir[^t-BuP,C,P^{Fe}], the palladium atom deviates from the cyclopentadienyl plane by a larger distance, 0.361 Å. The reason for this is a larger size of the BH₄[−] group as compared to that of the chlorine atom. A comparable deviation (0.358 Å) of the overcrowded Ir atom is observed in octahedral complex **20** (vide supra). Obviously, a similar deviation of the chelated iridium atom can occur upon formation of intermediates involved in a catalytic cycle of alkane

dehydrogenation with the participation of Ir[^t-BuP,C,P^{Ru}] and, to a larger extent, Ir[^t-BuP,C,P^{Fe}] species. Therefore, it can also influence the stability of complexes IrH₂(alkene)[^t-BuP,C,P^M] and Ir(alkene)[^t-BuP,C,P^M] and, as a result, the overall dehydrogenation reaction rate.

As for electronic effects of the Ir[P,C,P] fragments, the ν_{CO} values indicate that the effect of metallocene-based fragments Ir[^t-BuP,C,P^M] is close to that of Ir[^t-BuP,C,P] containing a benzene-based bis(phosphine) ligand. The ¹⁹F NMR data for *m*- and *p*-fluorophenyl-substituted cyclopentadienyl compounds reveal that electronic effects of the ferrocenyl and ruthenocenyl groups as substituents are close to that of alkyl groups.²² At the same time, in the series ferrocenyl, ruthenocenyl, and osmocenyl, the σ component of the overall electron-donating effect of the metallocenyl group successively increases and the π component decreases.^{22c} Therefore, the ligand ^t-BuP,C,P^{Fe} may be somewhat more π -electron-donating than ^t-BuP,C,P^{Ru}.

Thus, a great number of factors, both steric and electronic, are responsible for the catalytic activity of iridium pincer complexes **6** and **7**. For the first time, we draw attention to the fact that the value of the P–Ir–P angle in pincer complexes may determine to a large extent the catalytic properties of these systems. Another steric factor, intrinsic only for metallocene-based pincer complexes, originates from a close contact of the pseudoequatorial organyl groups at the P atoms and the nonmetalated cyclopentadienyl ring. Exploration of this peculiarity by derivatization of a nonmetalated cyclopentadienyl ring may allow fine-tuning of the catalytic activity and selectivity of metallocene-based pincer complexes.

Concluding Remarks

When we began studies of metallocene-based pincer complexes, our aim was the development of homogeneous catalytic systems for alkane dehydrogenation relative to known benzene-based pincer complexes of iridium.⁴ We wished to answer three questions: whether it is possible to prepare metallocene-based P,C,P pincer complexes, whether these complexes will be sufficiently stable thermally for their use in catalysis (bearing in mind strong ring strain in the fused five-membered metalacycles), and whether the iridium pincer complexes IrH₂-[^RP,C,P^M] catalyze alkane dehydrogenation. As is seen from this and earlier papers,^{7,12} positive answers to all these questions were obtained. We have also demonstrated that binuclear complexes **6** and **7** are the most active among all known homogeneous catalysts for alkane transfer dehydrogenation.

The sandwich nature of metallocene-based pincer ligands opens new horizons for the creation of transition metal complexes with fine-tunable catalytic properties.

Experimental Section

General Considerations. All experiments with metal complexes and phosphine ligands were carried out under purified argon atmosphere using standard Schlenk techniques. All solvents were reagent grade or better. Solvents were refluxed over sodium/benzophenone ketyl and distilled under an argon atmosphere.

(19) Dunitz, J. D.; Orgel, L. E.; Rich, A. *Acta Crystallogr.* **1956**, *9*, 373–375.

(20) Hardgrave, G. L.; Templeton, D. H. *Acta Crystallogr.* **1959**, *12*, 28–32.

(21) Kuklin, S. A.; Dolgushin, F. M.; Petrovskii, P. V.; Koridze, A. A. *Russ. Chem. Bull., Int. Ed.*, submitted.

(22) (a) Koridze, A. A.; Gubin, S. P.; Lubovich, A. A.; Kvasov, B. A.; Ogorodnikova, N. A. *J. Organomet. Chem.* **1971**, *32*, 273–277. (b) Ogorodnikova, N. A.; Koridze, A. A.; Gubin, S. P. *J. Organomet. Chem.* **1981**, *215*, 293–301. (c) Gubin, S. P.; Koridze, A. A.; Ogorodnikova, N. A.; Bezrukova, A. A.; Kvasov, B. A. *Izv. Akad. Nauk, Ser. Khim.* **1981**, 1170–1172. (d) Bitterwolf, T. E.; Ling, A. C. *J. Organomet. Chem.* **1977**, *141*, 355–370.

Deuterated solvents were degassed with argon. Commercially available reagents were used as received. Complexes $[\text{Ir}(\text{COE})_2\text{Cl}]_2$,²³ 1-(ethoxycarbonyl)-3-formylferrocene²⁴ and -ruthenocene,²⁴ and diphosphine $[\text{t-BuP}, \text{CH}, \text{P}^{\text{Fe}}]_2$ ^{7a} were prepared according to literature procedures.

¹H, ¹¹B, ¹³C, ¹⁹F, and ³¹P NMR spectra were recorded at 400.13, 128.38, 100.61, 282.40, and 161.98 MHz, respectively, using a Bruker AMX-400 NMR spectrometer. ¹H and ¹³C{¹H} NMR chemical shifts are reported in parts per million downfield from tetramethylsilane. ¹H NMR chemical shifts were referred to the residual hydrogen signal of the deuterated solvents. In ¹³C{¹H} NMR measurements the signal of C₆D₆ (128.0 ppm) was used as a reference. ¹¹B NMR chemical shifts are reported relative to external BF₃·Et₂O. ¹⁹F NMR chemical shifts are reported relative to external CFCl₃. ³¹P NMR chemical shifts are reported in parts per million downfield from H₃PO₄ and referred to an external 85% solution of phosphoric acid in D₂O. FTIR spectra were recorded on a Nicolet Magna-IR 750 Fourier spectrometer; mass spectra were measured on a Finnigan LCQ instrument. Catalytic reactions were monitored using a Perkin-Elmer F22 gas chromatograph with a 50 m × 0.2 mm i.d. × 0.33 μm Hewlett-Packard quartz capillary column with methylsiloxane. Elemental analyses were performed at the A.N. Nesmeyanov Institute of Organoelement Compounds of RAS. NIR spectra were recorded on a JSD-205 Fourier spectrometer. Band parameters of the NIR spectra were determined by a curve fit procedure.

Synthesis of {1,3-(HOCH₂)₂C₅H₃}Ru(C₅H₅). A solution of 1-(ethoxycarbonyl)-3-formylruthenocene²⁴ (1.5 g, 4.53 mmol) in diethyl ether (100 mL) was added dropwise to a suspension of LiAlH₄ (1.5 g, 39.5 mmol) in ether (75 mL). The solution was stirred at room temperature for 4 h. Then water was added, and the aqueous layer was separated and extracted several times with ether (3 × 100 mL). The combined etherial solutions were dried over Na₂SO₄. The solvent was removed under vacuum, giving pure product. Yield: 1 g (72%). ¹H NMR (CDCl₃): δ 1.32 (t, *J*_{H-H} = 5.5 Hz, 2H, OH), 4.00 (d, *J*_{H-H} = 5.5 Hz, 4H, CH₂), 4.62 (s, 5H, C₅H₅), 4.63 (d, *J*_{H-H} = 1.2 Hz, 2H, H(4,5)), 4.76 (t, *J*_{H-H} = 1.2 Hz, 1H, H(2)). Anal. Calcd for C₁₂H₁₄O₂Ru: C, 49.49; H, 4.81. Found: C, 48.78; H 5.03.

Synthesis of [t-BuP,CH,P^{Ru}] (13). t-BuPH (0.50 mL, 410 mg, 2.82 mmol) was added to a solution of 1,3-bis(hydroxymethyl)-ruthenocene (410 mg, 1.41 mmol) in acetic acid (20 mL). The solution was stirred at 80 °C for 3 h. The solvent was removed under vacuum, and the residue was dried under vacuum (heating 100 °C). The crude product was dissolved in a small amount of dichloromethane, a large amount of methanol was added, and the solution was cooled to -20 °C for 12 h. The cold supernatant was removed, and the solid was washed with methanol and dried under vacuum. Yield: 380 mg (50%). Some additional quantity of the product was recovered by evaporation of supernatant solution and additional crystallization. ³¹P{¹H} NMR (CDCl₃): δ 34.08 (s, 2P). ¹H NMR (CDCl₃): δ 1.17–1.20 (m, 36H, C(CH₃)₃), 2.65 (br s, 4H, CH₂), 4.63 (s, 5H, C₅H₅), 4.83 (s, 2H, C₅H₂). MS: *m/z* 548 (M⁺). Anal. Calcd for C₂₈H₄₈P₂Ru: C, 61.43; H, 8.87. Found: C, 62.06; H, 9.08.

Reaction of [Ir(COE)₂Cl]₂ with 10. Formation of H-endo- (11) and H-exo-IrH(Cl)[t-BuP,CH,P^{Fe}] (12). [Ir(COE)₂Cl]₂ (319 mg, 0.356 mmol) was added to a solution of 1,3-bis((di-*tert*-butylphosphino)methyl)ferrocene (10) (358 mg, 0.713 mmol) in 30 mL of toluene. Then 50 mL of toluene was added. The mixture was refluxed with stirring for 10 h. Then additional [Ir(COE)₂Cl]₂ (40–50 mg) was added, and the solution was refluxed for another 8 h. The solvent was removed in vacuo, the oily residue was dissolved

in a small amount of dichloromethane, and the solution was diluted with hexane and evaporated. A solid precipitate was extracted with hexane until the extract became colorless. The hexane extract was evaporated to a small volume (4–6 mL) and cooled. The precipitated product was washed with a small volume of hexane and dried in a vacuum at room temperature. Yield: 363 mg (70%). According to the NMR spectra, the product is a mixture of **11** and **12** in a ratio of ~2:5.

Characterization of 11. ³¹P{¹H} NMR (CDCl₃): δ 79.62 (s, 2P). ¹H NMR (CDCl₃): δ -43.54 (t, *J*_{P-H} = 13.32 Hz, 1H, Ir-H), 1.23 (vt, *J*_{P-H} = 6.7 Hz, 18H, C(CH₃)₃), 1.53 (vt, *J*_{P-H} = 6.7 Hz, 18H, C(CH₃)₃), 2.76 (dt, *J*_{H-H} = 17.2 Hz, *J*_{P-H} = 4.0 Hz, 2H, CH_AH_BP), 3.06 (dt, *J*_{H-H} = 17.2 Hz, *J*_{P-H} = 4.0 Hz, 2H, CH_AH_BP), 4.37 (s, 2H, C₅H₂), 4.54 (s, 5H, C₅H₅).

Characterization of 12. ³¹P{¹H} NMR (CDCl₃): δ 87.62 (s, 2P). ¹H NMR (CDCl₃): δ -39.48 (t, *J*_{P-H} = 13.8 Hz, 1H, Ir-H), 1.99 (vt, *J*_{P-H} = 6.7 Hz, 18H, C(CH₃)₃), 1.59 (vt, *J*_{P-H} = 6.7 Hz, 18H, C(CH₃)₃), 2.78 (dt, *J*_{H-H} = 17.2 Hz, *J*_{P-H} = 4.0 Hz, 2H, CH_AH_BP), 2.87 (dt, *J*_{H-H} = 17.2 Hz, *J*_{P-H} = 4.0 Hz, 2H, CH_AH_BP), 3.78 (s, 2H, C₅H₂), 3.86 (s, 5H, C₅H₅). MS: *m/z* 729.5 (M⁺). Anal. Calcd for C₂₈H₄₈ClFeIrP₂: C, 46.06; H, 6.58. Found: C, 47.16; H, 6.80.

Isomerization of 11 into 12. Heating of a 1:1 mixture of **11** and **12** (30 mg) in refluxing cyclooctane (8 mL) for 8 h results in quantitative formation of H-*exo* isomer **12** without any sign of product decomposition (³¹P{¹H} and ¹H NMR analysis).

Reaction of [Ir(COE)₂Cl]₂ with 13. Formation of H-endo- (14) and H-exo-IrH(Cl)[t-BuP,CH,P^{Ru}] (15). The reaction was performed as described above for diphosphine **10**. Yield: 29%.

Characterization of 14. ³¹P{¹H} NMR (CD₂Cl₂): δ 79.50 (s, 2P). ¹H NMR (CD₂Cl₂): δ -44.42 (t, *J*_{P-H} = 13.0 Hz, 1H, Ir-H), 1.27 (vt, *J*_{P-H} = 7.2 Hz, 18H, C(CH₃)₃), 1.39 (vt, *J*_{P-H} = 7.2 Hz, 18H, C(CH₃)₃), 2.62–2.81 (m, 4H, CH₂), 4.18 (s, 5H, C₅H₅), 4.71 (s, 2H, C₅H₂).

Characterization of 15. ³¹P{¹H} NMR (CD₂Cl₂): δ 87.20 (s, 2P). ¹H NMR (CD₂Cl₂): δ -38.28 (t, *J*_{P-H} = 13.9 Hz, 1H, Ir-H), 1.23 (vt, *J*_{P-H} = 7.2 Hz, 18H, C(CH₃)₃), 1.46 (vt, *J*_{P-H} = 7.2 Hz, 18H, C(CH₃)₃), 2.61–2.76 (m, 4H, CH₂), 4.29 (s, 5H, C₅H₅), 4.88 (s, 2H, C₅H₂). Anal. Calcd for C₂₈H₄₈ClIrP₂Ru: C, 43.38; H, 5.68. Found: C, 43.19; H, 5.41.

Formation of {H-*exo*-IrH(Cl)[t-BuP,CH,P^{Fe}]}BAR₄^F (18). Complex [Cp₂Fe]BAR₄^F (77.5 mg, 0.074 mmol) was added to a stirred solution of **12** (54 mg, 0.074 mmol) in dichloromethane (6 mL). The solution was stirred for 1 h, the solvent was removed under vacuum, and the residue was washed twice with benzene. The solid was dissolved in dichloromethane; hexane was added to this solution (the ratio CH₂Cl₂–hexane ~1:5) to cause precipitation. The solvents were removed by decantation, and the solid was washed twice, first with benzene and then with hexane, and dried under vacuum. Yield: 110 mg (93.2%).

When a mixture of **11** and **12** (in a ratio of ~2:5) was treated with [Cp₂Fe]BAR₄^F under the same conditions, isomeric cationic complexes **17** and **18** were generated.

Characterization of 17. ³¹P{¹H} NMR (CD₂Cl₂): δ 49.11 (s, 2P). ¹H NMR (CD₂Cl₂): δ -115.3 (br, 2H, CH_AH_BP), -68.83 (br, 2H, CH_AH_BP), -5.73 (br, 18H, C(CH₃)₃), 7.57 (s, 18H, C(CH₃)₃), 18.60 (br, 5H, C₅H₅), 34.66 (br, 2H, C₅H₂). ¹¹B NMR (CD₂Cl₂): δ -8.92 (s). ¹⁹F NMR (CD₂Cl₂): δ 16.72 (s).

Characterization of 18. ³¹P{¹H} NMR (CD₂Cl₂): δ 54.39 (s, 2P). ¹H NMR (CD₂Cl₂): δ -126.08 (br, 2H, CH_AH_BP), -63.33 (br, 2H, CH_AH_BP), -6.75 (br, 18H, C(CH₃)₃), 7.73 (s, 18H, C(CH₃)₃), 18.46 (br, 5H, C₅H₅), 40.58 (br, 2H, C₅H₂). ¹¹B NMR (CD₂Cl₂): δ -8.92 (s). ¹⁹F NMR (CD₂Cl₂): δ 16.72 (s). Anal. Calcd for C₆₀H₅₆BClF₂₄FeIrP₂: C, 45.26; H, 3.51; F, 28.66. Found: C, 45.38; H, 3.56; F, 28.25.

Reaction of Carbon Monoxide with 11 and 12. Carbon monoxide was bubbled through a solution of a mixture of **11** and

(23) van der Ent, A.; Onderdelenden, A. L. *Inorg. Synth.* **1990**, 28, 91–92.

(24) Bickert, P.; Hildebrandt, B.; Hafner, K. *Organometallics* **1984**, 3, 653–657.

12 (in ~2:5 ratio) (50 mg, 0.068 mmol) in benzene (10 mL) for 15 min. The dark red solution immediately turned yellow-brown. The reaction was monitored by ^1H and $^{31}\text{P}\{^1\text{H}\}$ NMR. The reaction mixture contained isomeric complexes H-*endo*- (**19**) and H-*exo*-IrH(Cl)(CO)[$^t\text{-BuP,C,P}^{\text{Fe}}$] (**20**) and a small amount of Ir(CO)-[$^t\text{-BuP,C,P}^{\text{Fe}}$] (**21**) (identified by comparison of the spectral data with those for the authentic sample). The solvent was removed in vacuo, and the resulting powder was crystallized from a hexane–benzene mixture, yielding **19** and **20** (20.5 mg, 60%). The major isomer **20** was obtained in analytically pure form and fully characterized.

Characterization of 19. $^{31}\text{P}\{^1\text{H}\}$ NMR (C_6D_6): δ 71.28 (s, 2P). ^1H NMR (C_6D_6): δ -6.59 (t, $J_{\text{P-H}} = 14.3$ Hz, 1H, Ir-H), 1.43 (vt, $J_{\text{P-H}} = 6.8$ Hz, 18H, C(CH_3)₃), 1.64 (vt, $J_{\text{P-H}} = 6.8$ Hz, 18H, C(CH_3)₃), 2.62 (dt, $J_{\text{H-H}} = 16.8$ Hz, $J_{\text{P-H}} = 4.8$ Hz, 2H, $\text{CH}_\text{A}\text{H}_\text{B}\text{P}$), 2.92 (dt, $J_{\text{H-H}} = 16.8$ Hz, $J_{\text{P-H}} = 3.8$ Hz, 2H, $\text{CH}_\text{A}\text{H}_\text{B}\text{P}$), 3.92 (s, 5H, C_5H_5), 4.33 (s, 2H, C_5H_5). IR (CH_2Cl_2): 2025 cm^{-1} (ν_{CO}).

Characterization of 20. $^{31}\text{P}\{^1\text{H}\}$ NMR (C_6D_6): δ 66.72 (s, 2P). ^1H NMR (C_6D_6): δ -8.62 (t, $J_{\text{P-H}} = 15.2$ Hz, 1H, Ir-H), 1.24 (vt, $J_{\text{P-H}} = 6.8$ Hz, 18H, C(CH_3)₃), 1.57 (vt, $J_{\text{P-H}} = 6.8$ Hz, 18H, C(CH_3)₃), 2.31 (dt, $J_{\text{H-H}} = 16.4$ Hz, $J_{\text{P-H}} = 2.8$ Hz, 2H, $\text{CH}_\text{A}\text{H}_\text{B}\text{P}$), 2.84 (dt, $J_{\text{H-H}} = 16.4$ Hz, $J_{\text{P-H}} = 2.8$ Hz, 2H, $\text{CH}_\text{A}\text{H}_\text{B}\text{P}$), 4.07 (s, 2H, C_5H_5), 4.16 (s, 5H, C_5H_5). IR (CH_2Cl_2): 1997 cm^{-1} (ν_{CO}). Anal. Calcd for $\text{C}_{29}\text{H}_{48}\text{ClFeIrOP}_2$: C, 45.94; H, 6.34. Found: C, 46.20; H, 6.40.

Formation of Ir(CO)[$^t\text{-BuP,C,P}^{\text{Fe}}$] (21**).** A mixture of **11** and **12** (in a ~2:5 ratio) (60 mg, 0.082 mmol) and sodium hydride (50 mg, 2.083 mmol) in cyclooctane (10 mL) was refluxed for 1 h. After cooling, carbon monoxide was bubbled through the solution for 0.5 h. The reaction mixture was filtered through Celite, the solvent was removed under vacuum, and the residue was crystallized from hexane. Yield: 36.8 mg (62%). $^{31}\text{P}\{^1\text{H}\}$ NMR (C_6D_6): δ 99.36 (s, 2P). ^1H NMR (C_6D_6): δ 1.25 (vt, $J_{\text{P-H}} = 6.4$ Hz, 18H, C(CH_3)₃), 1.50 (vt, $J_{\text{P-H}} = 6.4$ Hz, 18H, C(CH_3)₃), 2.75 (dt, $J_{\text{H-H}} = 16.4$ Hz, $J_{\text{P-H}} = 2.4$ Hz, 2H, $\text{CH}_\text{A}\text{H}_\text{B}\text{P}$), 3.14 (dt, $J_{\text{H-H}} = 16.4$ Hz, $J_{\text{P-H}} = 2.4$ Hz, 2H, $\text{CH}_\text{A}\text{H}_\text{B}\text{P}$), 4.07 (s, 5H, C_5H_5), 4.44 (s, 2H, C_5H_5). $^{13}\text{C}\{^1\text{H}\}$ NMR (C_6D_6): δ 29.22 (vt, $J_{\text{P-C}} = 14.4$ Hz, 2C, CH_2P), 29.59 (vt, $J_{\text{P-C}} = 3.4$ Hz, 6C, C(CH_3)₃), 29.87 (vt, $J_{\text{P-C}} = 3.4$ Hz, 6C, C(CH_3)₃), 35.93 (vt, $J_{\text{P-C}} = 9.0$ Hz, 2C, C(CH_3)₃), 36.84 (vt, $J_{\text{P-C}} = 10.0$ Hz, 2C, C(CH_3)₃), 65.52 (vt, $J_{\text{P-C}} = 6.4$ Hz, 2C, C(3,4)), 70.16 (s, 5C, C_5H_5), 94.40 (vt, $J_{\text{P-C}} = 13.4$ Hz, 2C, C(2,5)), 131.4 (t, $J_{\text{P-C}} = 6.0$ Hz, 1C, C(1)), 199.70 (t, $J_{\text{P-C}} = 6.8$ Hz, 1C, CO). IR (CH_2Cl_2): 1904 cm^{-1} (ν_{CO}). Anal. Calcd for $\text{C}_{29}\text{H}_{47}\text{FeIrOP}_2$: C, 48.27; H, 6.52. Found: C, 48.54; H, 6.51.

Formation of Ir(CO)[$^t\text{-BuP,C,P}^{\text{Ru}}$] (23**).** This complex was obtained by the procedure described above for **21** from a mixture of H-*endo*- (**14**) and H-*exo*-IrH(Cl)[$^t\text{-BuP,C,P}^{\text{Ru}}$] (**15**) (in a ~2:5 ratio) (26 mg, 0.036 mmol), NaH (40 mg, 1.67 mmol), and carbon monoxide. Yield: 19.6 mg (76%). $^{31}\text{P}\{^1\text{H}\}$ NMR (C_6D_6): δ 98.99 (s, 2P). ^1H NMR (C_6D_6): δ 1.29 (vt, $J_{\text{P-H}} = 7.2$ Hz, 18H, C(CH_3)₃), 1.37 (vt, $J_{\text{P-H}} = 7.2$ Hz, 18H, C(CH_3)₃), 2.80–2.94 (m, 4H, CH_2P), 4.47 (s, 5H, C_5H_5), 4.92 (s, 2H, C_5H_5). $^{13}\text{C}\{^1\text{H}\}$ NMR (C_6D_6): δ 29.06 (vt, $J_{\text{P-C}} = 14.4$ Hz, 2C, CH_2P), 29.67 (vt, $J_{\text{P-C}} = 3.2$ Hz, 6C, C(CH_3)₃), 29.96 (vt, $J_{\text{P-C}} = 3.2$ Hz, 6C, C(CH_3)₃), 35.57 (vt, $J_{\text{P-C}} = 10.0$ Hz, 2C, C(CH_3)₃), 36.81 (vt, $J_{\text{P-C}} = 10.0$ Hz, 2C, C(CH_3)₃), 68.80 (vt, $J_{\text{P-C}} = 6.4$ Hz, 2C, C(3,4)), 71.79 (s, 5C, C_5H_5), 102.45 (vt, $J_{\text{P-C}} = 13.6$ Hz, 2C, C(2,5)), 135.08 (t, $J_{\text{P-C}} = 6.0$ Hz, 1C, C(1)), 199.58 (t, $J_{\text{P-C}} = 6.8$ Hz, 1C, CO). IR (CH_2Cl_2): 1905 cm^{-1} (ν_{CO}). Anal. Calcd for $\text{C}_{29}\text{H}_{47}\text{IrOP}_2\text{Ru}$: C, 45.43; H, 6.14. Found: C, 45.63; H, 6.18.

Formation of [Ir(CO)[$^t\text{-BuP,C,P}^{\text{Fe}}$]]PF₆ (24**).** This compound was obtained by the procedure described for **18** from **21** (15 mg, 0.021 mmol) and [Cp₂Fe]PF₆ (6.8 mg, 0.021 mmol) in dichloromethane. Yield: 17 mg (94.4%). $^{31}\text{P}\{^1\text{H}\}$ NMR (CD_2Cl_2): δ 40.26 (s, 2P), -150.50 (sept, $J_{\text{P-F}} = 704.5$ Hz, 1P). ^1H NMR (CD_2Cl_2): δ -115.70 (br, 2H, $\text{CH}_\text{A}\text{H}_\text{B}\text{P}$), -43.57 (br, 2H, $\text{CH}_\text{A}\text{H}_\text{B}\text{P}$), -8.82 (s, 18H, C(CH_3)₃), 6.46 (s, 18H, C(CH_3)₃), 20.22 (br, 5H,

C_5H_5), 32.10 (br, 2H, C_5H_5). IR (CH_2Cl_2): 1951 cm^{-1} (ν_{CO}). Anal. Calcd for $\text{C}_{29}\text{H}_{47}\text{F}_6\text{FeIrOP}_3 \cdot 2\text{CH}_2\text{Cl}_2$: C, 35.91; H, 4.92. Found: C, 35.47; H, 4.53.

Formation of Ir(CN^{*t*}Bu)[$^t\text{-BuP,C,P}^{\text{Fe}}$] (25**) and IrH₂(CN^{*t*}Bu)-[$^t\text{-BuP,C,P}^{\text{Fe}}$] (**26**).** A mixture of H-*endo*- (**11**) and H-*exo*-IrH(Cl)-[$^t\text{-BuP,C,P}^{\text{Fe}}$] (**12**) (in ~2:5 ratio) (50 mg, 0.069 mmol) and sodium hydride (50 mg, 2.083 mmol) in cyclooctane (11 mL) was refluxed for 1 h. After cooling, the solution of IrH₂[$^t\text{-BuP,C,P}^{\text{Fe}}$] was decanted from the inorganic residue, and *tert*-butylisocyanide (0.2 mL, 0.147 g, 1.78 mmol) was added to the solution. The solvent was removed under vacuum, and the residue was crystallized from hexane. Yield: 45 mg (85%). According to the NMR, a mixture of **25** and **26** (~3:1) is formed. All attempts to separate these complexes by crystallization or chromatography were unsuccessful. However, the major product **25** may be isolated by fractional crystallization from hexane solution.

Characterization of 25. $^{31}\text{P}\{^1\text{H}\}$ NMR (C_6D_6): δ 94.92 (s, 2P). ^1H NMR (C_6D_6): δ 1.59 (s, 9H, CNC(CH_3)₃), 1.34 (vt, $J_{\text{P-H}} = 7.3$ Hz, 18H, C(CH_3)₃), 1.59 (vt, $J_{\text{P-H}} = 7.0$ Hz, 18H, C(CH_3)₃), 2.82 (dt, $J_{\text{H-H}} = 12.4$ Hz, $J_{\text{P-H}} = 4.1$ Hz, 2H, $\text{CH}_\text{A}\text{H}_\text{B}\text{P}$), 3.19 (dt, $J_{\text{H-H}} = 12.4$ Hz, $J_{\text{P-H}} = 1.5$ Hz, 2H, $\text{CH}_\text{A}\text{H}_\text{B}\text{P}$), 4.13 (s, 5H, C_5H_5), 4.54 (s, 2H, C_5H_5). IR (CH_2Cl_2): 2136 cm^{-1} (ν_{CN}). Anal. Calcd for $\text{C}_{33}\text{H}_{58}\text{FeIrNP}_2$: C, 51.06; H, 7.22. Found: C, 51.28; H, 7.30.

Characterization of 26. $^{31}\text{P}\{^1\text{H}\}$ NMR (C_6D_6): δ 83.90 (s, 2P). ^1H NMR (C_6D_6): δ -13.97 (dt, $J_{\text{H-H}} = 2.5$ Hz, $J_{\text{P-H}} = 16.4$ Hz, 1H, Ir-H), -11.37 (dt, $J_{\text{H-H}} = 2.5$ Hz, $J_{\text{P-H}} = 11.8$ Hz, 1H, Ir-H), 1.23 (s, 9H, CNC(CH_3)₃), 1.32 (vt, $J_{\text{P-H}} = 6.8$ Hz, 18H, C(CH_3)₃), 1.58 (vt, $J_{\text{P-H}} = 6.8$ Hz, 18H, C(CH_3)₃), 2.63 (dt, $J_{\text{H-H}} = 16.2$ Hz, $J_{\text{P-H}} = 4.4$ Hz, 2H, $\text{CH}_\text{A}\text{H}_\text{B}\text{P}$), 3.13 (dt, $J_{\text{H-H}} = 16.2$ Hz, $J_{\text{P-H}} = 1.5$ Hz, 2H, $\text{CH}_\text{A}\text{H}_\text{B}\text{P}$), 4.27 (s, 5H, C_5H_5), 4.36 (s, 2H, C_5H_5). IR (CH_2Cl_2): 2169 cm^{-1} (ν_{CN}).

Formation of Ir(CN^{*t*}Bu)[2,6-(^{*t*}Bu₂PO)₂C₆H₃] (27**) and IrH₂-(CN^{*t*}Bu)[2,6-(^{*t*}Bu₂PO)₂C₆H₃] (**28**).** A mixture of **27** and **28** in a ratio of ~5:1 was obtained by the procedure described above for **25** and **26**. Interaction of IrH(Cl)[2,6-(^{*t*}Bu₂PO)₂C₆H₃] (40 mg, 0.064 mmol) with sodium hydride (40 mg, 1.67 mmol) in cyclooctane (10 mL), with subsequent treatment of generated IrH₂[2,6-(^{*t*}Bu₂PO)₂C₆H₃] with *tert*-butylisocyanide (73.6 mg, 0.89 mmol), gave an inseparable mixture of **27** and **28**. Yield: 33 mg (76.1%). Complex **27** was isolated by fractional crystallization from hexane solution.

Characterization of 27. $^{31}\text{P}\{^1\text{H}\}$ NMR (C_6D_6): δ 193.91 (s, 2P). ^1H NMR (C_6D_6): δ 1.22 (s, 9H, CNC(CH_3)₃), 1.52 (vt, $J_{\text{P-H}} = 6.7$ Hz, 36H, 18H, C(CH_3)₃), 7.07 (m, 3H, C₆H₃). IR (CH_2Cl_2): 2052 cm^{-1} (ν_{CN}). Anal. Calcd for $\text{C}_{27}\text{H}_{48}\text{IrNO}_2\text{P}_2$: C, 48.21; H, 7.14. Found: C, 48.04; H, 7.07.

Characterization of 28. $^{31}\text{P}\{^1\text{H}\}$ NMR (C_6D_6): δ 161.31 (s, 2P). ^1H NMR (C_6D_6): δ -10.82 (t, $J_{\text{P-H}} = 16.8$ Hz, 2H, Ir-H), 0.98 (s, 9H, CNC(CH_3)₃), 1.61 (vt, $J_{\text{P-H}} = 7.3$ Hz, 36H, 18H, C(CH_3)₃), 7.07 (m, 3H, C₆H₃). IR (CH_2Cl_2): 2100 cm^{-1} (ν_{CN}).

Formation of IrH₂[$^t\text{-BuP,C,P}^{\text{Fe}}$] (6**).** A mixture of H-*endo*- (**11**) and H-*exo*-IrH(Cl)[$^t\text{-BuP,C,P}^{\text{Fe}}$] (**12**) (in ~2:5 ratio) (60 mg, 0.0822 mmol), sodium hydride (60 mg, 2.5 mmol), and cyclooctane (8 mL) was refluxed for 0.5 h. Then the reaction mixture was allowed to settle, the clean solution was decanted and evaporated, and the residue was dried under vacuum. Yield: 49 mg (85.8%). $^{31}\text{P}\{^1\text{H}\}$ NMR (C_6D_6): δ 102.63 (s, 2P). ^1H NMR (C_6D_6): δ -15.85 (t, $J_{\text{P-H}} = 7.6$ Hz, 2H, Ir-H), 0.8–1.8 (m, 36H, C(CH_3)₃), 2.91 (br dt, $J_{\text{H-H}} = 16.6$ Hz, $J_{\text{P-H}} = 3.6$ Hz, 2H, $\text{CH}_\text{A}\text{H}_\text{B}\text{P}$), 3.11 (br dt, $J_{\text{H-H}} = 16.6$ Hz, $J_{\text{P-H}} = 1.0$ Hz, 2H, $\text{CH}_\text{A}\text{H}_\text{B}\text{P}$), 4.10 (s, 5H, C_5H_5), 4.63 (s, 2H, C_5H_5).

Formation of IrH₂[$^t\text{-BuP,C,P}^{\text{Ru}}$] (7**).** This compound was obtained by the procedure described above for **6**, from a mixture of H-*endo*- (**14**) and H-*exo*-IrH(Cl)[$^t\text{-BuP,C,P}^{\text{Ru}}$] (**15**) (in ~2:5 ratio) (30 mg, 0.0387 mmol) and sodium hydride 24 mg (1 mmol) in cyclooctane (10 mL). Yield: 21 mg (73.3%). $^{31}\text{P}\{^1\text{H}\}$ NMR (C_6D_6): δ 102.36 (s, 2P). ^1H NMR (C_6D_6): δ -15.95 (t, $J_{\text{P-H}} =$

Table 3. Crystal Data, Data Collection, and Structure Refinement Parameters for **20**, **21**, and **30**

	20	21	30
formula	C ₂₉ H ₄₈ OP ₂ ClFeIr·C ₆ H ₆	C ₂₉ H ₄₇ OP ₂ FeIr	C ₂₃ H ₃₉ O ₃ P ₂ Ir
molecular weight	836.22	721.66	617.68
cryst color, habit	orange prism	red prism	orange prism
temperature, K	115(2)	295(2)	120(2)
cryst syst	monoclinic	monoclinic	triclinic
space group	<i>P</i> 2 ₁ / <i>c</i>	<i>P</i> 2 ₁ / <i>n</i>	<i>P</i> 1
<i>a</i> , Å	13.3714(8)	8.552(2)	8.2658(7)
<i>b</i> , Å	16.397(1)	18.948(5)	12.030(1)
<i>c</i> , Å	16.3690(9)	18.375(6)	13.400(1)
α, deg			100.742(2)
β, deg	94.351(1)	92.55(3)	96.022(2)
γ, deg			103.813(2)
<i>V</i> , Å ³	3578.6(4)	2975(1)	1255.6(2)
<i>Z</i>	4	4	2
<i>d</i> (calc), g cm ^{−3}	1.552	1.611	1.634
diffractometer	SMART 1000	CAD4	SMART 1000
scan mode	ω	θ−5/3θ	ω
θ _{max} , deg	29.0	28.0	28.0
μ (Mo Kα, λ = 0.71073 Å), cm ^{−1}	43.10	50.84	54.64
absorp corr	SADABS	ψ-scan	SADABS
<i>T</i> _{min} / <i>T</i> _{max}	0.168/0.433	0.519/0.999	0.185/0.398
no. unique reflns (<i>R</i> _{int})	9436 (0.0394)	7152 (0.0297)	5964 (0.0264)
no. obsd reflns (<i>I</i> > 2σ(<i>I</i>))	8312	5968	5424
<i>R</i> ₁ (on <i>F</i> for obsd reflns) ^a	0.0309	0.0251	0.0266
<i>wR</i> ₂ (on <i>F</i> ² for all reflns) ^b	0.0759	0.0660	0.0674
GOOF	1.025	1.020	1.049

$$^a R_1 = \sum |F_o| - |F_c| / \sum |F_o|. \quad ^b wR_2 = \{\sum [w(F_o^2 - F_c^2)^2] / \sum w(F_o^2)^2\}^{1/2}.$$

7.6 Hz, 2H, Ir-*H*₂), 0.57–2.00 (m, 36H, C(CH₃)₃), 3.10 (br d, *J*_{H–H} = 16.6 Hz, 2H, CH_AH_BP), 3.31 (br d, *J*_{H–H} = 16.6 Hz, 2H, CH_AH_BP), 4.52 (s, 5H, C₅H₅), 5.13 (s, 2H, C₅H₂).

Formation of IrH₄[¹-BuP,C,P^{Fe}] (22**).** Complex **22** was obtained upon treatment of a pentane solution (100 mL) of **12** (150 mg, 0.2056 mmol) with 1.2 atm of hydrogen for 1 h, addition of ~2 mL of a saturated ethereal solution of LiAlH₄, and further bubbling of hydrogen through the solution for 1 h. The yellow solution of the tetrahydride **22** was cooled to −78 °C and then filtered through Celite, the solvent was removed at ambient temperature in the stream of hydrogen, and the residue was extracted with pentane; the extract was again evaporated by the method described above. The residue, complex **22**, is extremely sensitive to air and moisture. ³¹P{¹H} NMR (toluene-*d*₈): δ 85.28 (s, 2P). ¹H NMR (C₆D₆): δ −6 to −11.5 (br m, 4H, Ir-*H*₄), 1.1–1.7 (m, 36H, C(CH₃)₃), 2.52 (br d, *J*_{H–H} = 16.5 Hz, 2H, CH_AH_BP), 3.19 (br d, *J*_{H–H} = 16.5 Hz, 2H, CH_AH_BP), 4.23 (s, 5H, C₅H₅), 4.79 (s, 2H, C₅H₂).

General Procedure for the Transfer Dehydrogenation of COA with TBE. Stock solutions were prepared by stirring cyclooctane, the respective chloro-hydrido complex IrH(Cl)-[¹-BuP,C,P^M] (M = Fe, **12**; M = Ru, **15**) or IrH(Cl)[2,6-(¹-Bu₂-PO)₂C₆H₃], and sodium hydride at 151 °C for 1 h. After cooling, the solution was left to settle. Aliquots of these solutions were transferred into 4 mL thick walled Kontes reactors closed with Teflon screw caps, *tert*-butylethylene was added (the molar ratio of COA/TBE was 1:1), and the reactors were placed in an oil bath heated to 180 °C. After the desired reaction time, the reactors were cooled by a stream of air. The aliquots of the reaction mixtures were analyzed by GC. No signals other than COA, COE, TBE,

and TBA were detected in these reaction mixtures. An average of three runs of the stock solutions was taken in order to determine the TON at a given reaction time.

In a typical experiment, 26.770 g of cyclooctane (257.03 mmol), 9 mg of IrH(Cl)[¹-BuP,C,P^{Fe}] (**12**) (12.326 μmol), and 10 mg of sodium hydride (0.375 mmol) were stirred at 151 °C for 1 h. After cooling, 1.5 mL aliquot portions of the stock solutions were transferred into a Kontes reactor, 1 equiv of TBE was added (COA/TBE molar ratio was 1:1), and the reactor was placed in an oil bath heated to 180 °C for 8 h.

X-ray Diffraction Study. X-ray-quality crystals of **20**, **21**, and **30** were grown by slow crystallization of samples from CH₂Cl₂–benzene, hexane, and benzene solutions, respectively. Details of the crystal data, data collection, and structure refinement parameters are given in Table 3. Data were corrected for absorption effect. The structures have been solved by direct methods and refined by the full-matrix least-squares technique against *F*² with the anisotropic temperature parameters for all non-hydrogen atoms. The hydride ligand in complex **20** was located from the Fourier synthesis and refined in isotropic approximation. The remaining hydrogen atoms in structures **20**, **21**, and **30** were placed geometrically and included in the structure factor calculation in the riding motion approximation. The SHELXTL-97 program package²⁵ was used throughout the calculations.

Supporting Information Available: X-ray crystallographic data for **20**, **21**, and **30** as a CIF file. This material is available free of charge via the Internet at <http://pubs.acs.org>.

OM060715W

(25) Sheldrick, G. M. *SHELXTL-97*, version 5.10; Bruker AXS Inc.: Madison, WI, 1997.